Electronic Supplementary Material (ESI) for Analytical Methods.

Supplemental

Preparation of SNAP stock solutions

The reaction of producing NO from SNAP is based on equation S1 from Zhang et al (2004). The final concentration of NO in equilibrium with SNAP in the solution is described by equation S1:

$$2RSNO \rightarrow 2NO + RS - SR \qquad \textbf{(Equation S1)}$$

A saturated cuprous chloride solution (2.4 mM CuCl) was prepared in deoxygenated (argon purged) DI water. In a separate container, stock SNAP solution was prepared separately as follows: EDTA (53.7 µM) was adjusted to pH 9.0 using NaOH. The EDTA solution was then deoxygenated using argon purging, and SNAP was added and vortex mixed (total SNAP concentration 0.1 mM).

Abiotic NO transport studies

Calibrated NO microsensors were used to measure flux in the SR modality. The SR microsensor technique is a non-invasive modality that measures flux within the concentration boundary layer. SR uses computer-controlled translation of the microelectrode between two positions separated by a known distance (dX). Differential concentration (dC) is recorded in real time and flux is then calculated using Fick's first law of diffusion ($J=-D*dC*dX^{-1}$); where J= NO flux [nmol cm^{-2} sec^{-1}], D= diffusion constant of NO [cm^2 sec^{-1}], dC= NO concentration differential [nM], and dX= microelectrode oscillation distance [µm]. See McLamore and Porterfield [25] for a detailed review of the technique. To prepare a stable abiotic NO concentration gradient for the abiotic transport studies, two different NO donor-polymer composites were injected into

a source pipette based on McLamore et al [32] and Koehler et al [27]. The polymers used in this study were chitosan, the major structural component of *Artemia* cyst shells as described by Tajik et al [33], and alginate hydrogel, which has been used extensively as a material that mimics some of the properties of bacterial biofilms and tissues [34,35].

Chitosan and alginate hydrogels were prepared according to Burrs et al [36]. NO stock solutions of 1 mM MAHMA NONOate were prepared in PBS, pH 7.3 and stored immediately when not in use at -80°C. Composites of polymer and NO donor were prepared by mixing 1 mM stock NO donor solution with the polymer, vortex agitating for 30 sec, and then immediately backfilling into a tapered borosilicate glass pipette (open diameter was 200μm). The tapered pipette containing NO donor and polymer was immediately placed into a 3D micromanipulator (World precision Instruments, Sarasota, FL) with a resolution of 0.1 μm and immersed in PBS buffer. A calibrated NO microelectrode was positioned within 1 μm of the gel surface and flux was recorded based on the methods in McLamore et al [31,37]. For all abiotic transport studies, NO concentration within 5 μm of the source pipette was validated using UV absorbance at 337 nm with a fiber optic UV spectrometer (Ocean Optics, Dunedin, FL) based on Koehler et al [27].

A diffusion model was developed based on Koehler et al [27] using **Equation 2**. NO diffusion coefficients vary considerably in different media, which can significantly affect flux data. For example, Koehler et al [27] report a value of D (3.3×10^{-5} cm^2 s^{-1}) that is significantly higher than the value reported by Zacharia and Deen [38]; which is $2.21 \times 10^{-}$

^{5} cm^{2} s^{-1}. To determine the effective diffusion coefficient (D_{eff}) in the polymer composite and conditions tested here, the deterministic model was used to calculate D_{eff} from empirical data by minimizing the Chi^{2}.

$$C(x) = \frac{C_o R_o}{x} e^{\frac{-k*(r-R_o)}{2D_{eff}}} \quad \text{(Equation 2)}$$

where: x= distance from tip of source pipette [μm]; C_o= concentration of NO in source pipette [120 nM]; R_o= radius of source pipette [200 μm]; k= rate constant for NO in solution [12 msec^{-1}].

Table S1. Selectivity of rGO-nPt-nCe microelectrode toward ascorbic acid (AA) and nitrite (NO_2) in PBS (pH=7.2) at 25°C and + 720 mV versus Ag/AgCl.

Compound	Average Faradaic current [pA]	Selectivity ratio
NO (10nM)	32.91 ± 0.29	-
NO (100nM)	114.06 ± 10.23	-
AA (10nM)	0.06 ± 0.01	600
AA (100nM)	0.15 ± 0.12	765
NO_2 (10nM)	0.04 ± 0.01	900
NO_2 (100nM)	0.121 ± 0.05	940

Table 1. Comparison of NO-selective electrochemical microelectrodes (tip size smaller than 100 μm) within the last 15 years in terms of response time, sensitivity, operating potential, and limit of detection.

	Coating	**Potent. [mV]**	**Diam. [μm]**	**Res. time [sec]**	**Sensitivity (pA nM^{-1})**	**LOD (nM)**	**Reference**
Carbon fiber	WPI membrane[a]	+865	0.1	3±NR	0.5±NR pA nM^{-1}	2.0±NR[b]	Zhang et al (2002)
	Nafion and cellulose acetate	+870	6	4±NR	0.3±NR pA nM^{-1}	1000±NR	Katrlık et al (2002)
	Nickel	+830	7	≈30±NR	0.8±NR pA nM^{-1}	1.5±NR	Hrbác et al

	porphyrin						(2006)
Pt electrode	Nafion and WPI membrane[a]	+865	50	10±NR	5.8±NR pA nM^{-1}	2.1±NR	Dickson et al. (2004)
	Nano Pt	+ 750	150	25±NR	0.8±NR pA nM^{-1}	0.1±NR	Lee et al (2004)
	Nano Pt	+850	25	14±NR	0.4±0.1 pA nM^{-1}	1.0±NR	Lee et al (2007)
	Permiselective fluorine modified xerogel	+800	20	3±NR	7.9±NR pA nM^{-1}	0.1±NR	Shin et al (2008)
	Nanoceria-graphene composite, Nafion, OPD	+720	2	1.1±0.1	0.95±0.1 pA nM^{-1}	0.9±0.3	This work

[a]material details patented by World Precision Instruments
[b]SNR of 2 was used to calculate LOD value
NR = not reported

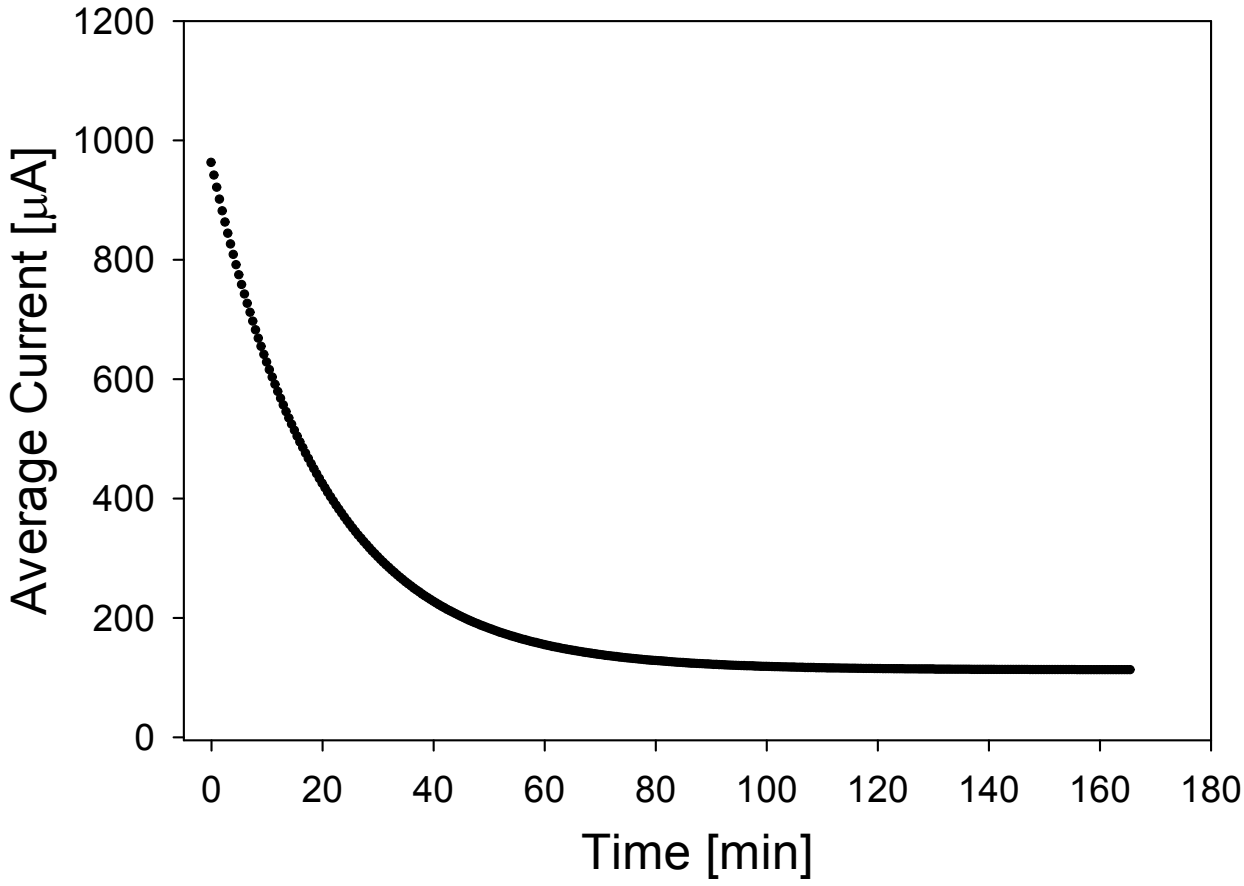

Figure S1. Representative current during deposition of OPD membrane at +900 mV in a solution of 5mM OPD and 0.1 mM AA. The deposition time in Figure S1 considerably shorter than the time required for deposition onto carbon fibers (4 hr) (Friedemann et al. 1996; Koehler et al. 2008; Porterfield et al. 2001).

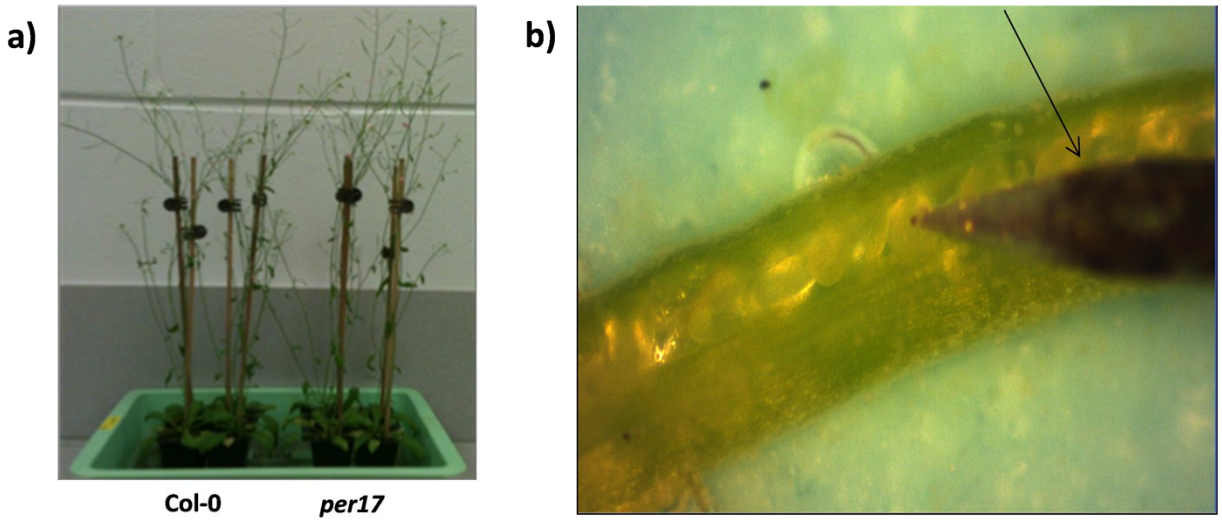

Figure S2. **a)** Photograph of Wild type (Col-0) and per17 mutants after 37 days of growth. **b)** Photograph of SR NO microsensor near the surface of *A. thaliana* ovules after opening of the silique wall. Arrow indicates electrode.

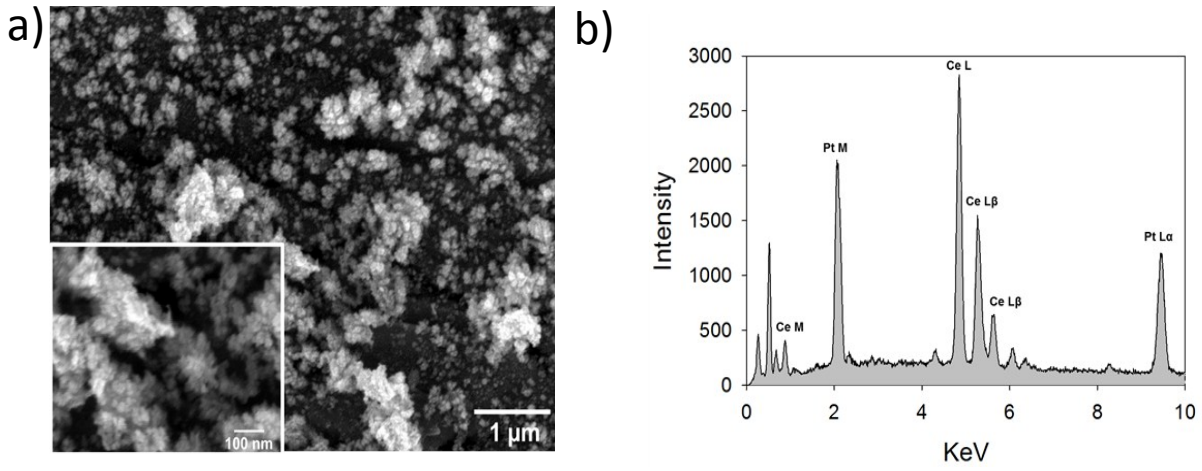

Figure S3. Material characterization of graphene-metal hybrid nanocomposite (courtesy of Chaturvedi et al., 2014). **a)** Scanning electron micrograph shows 20 nm nanoceria aggregates on the graphene-nPt surface (inset shows expanded view). **b)** Electron dispersive x-ray spectrograph confirm the presence of both cerium and platinum in the upper layers of the hybrid nanocomposite before deposition of Nafion and OPD.

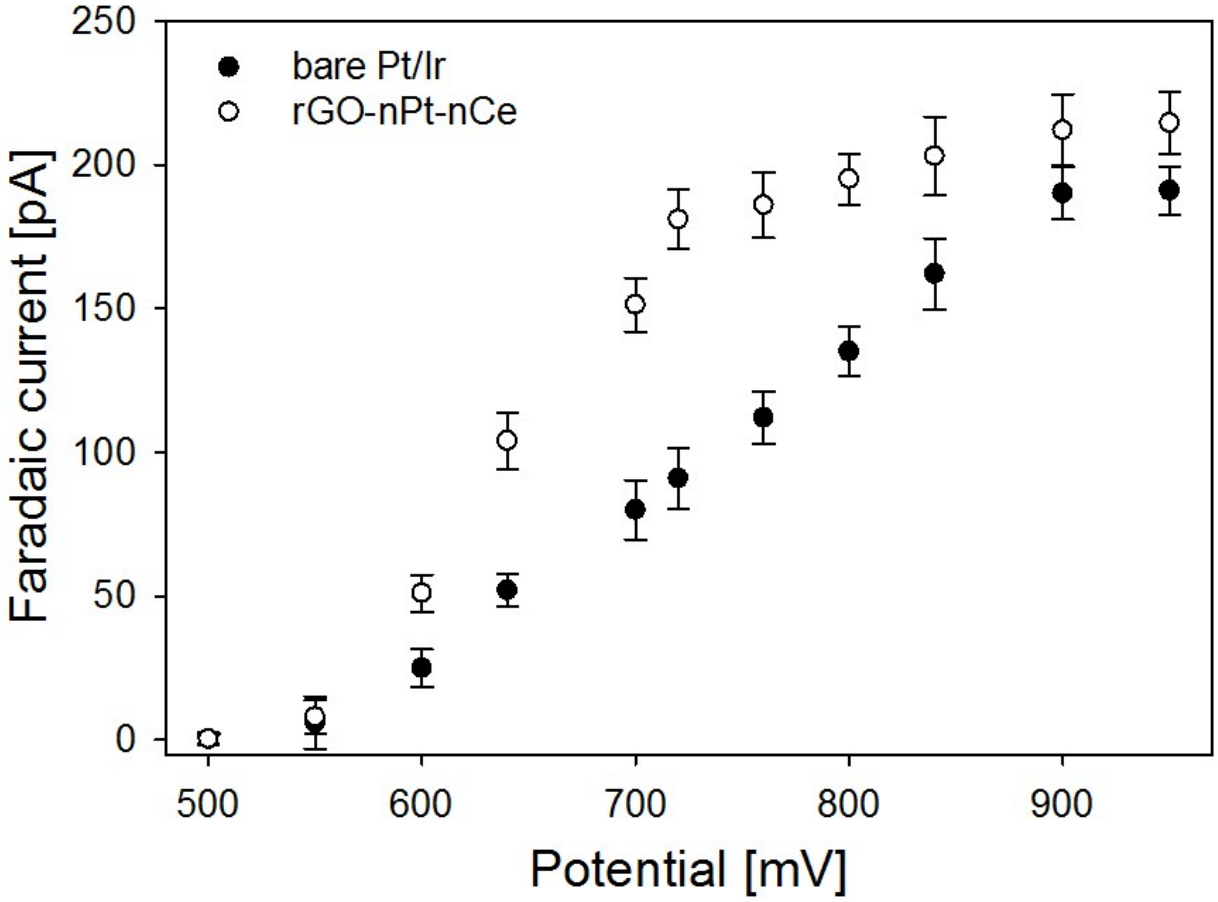

Figure S4. Steady state Faradaic current in the presence of 100 nM NO in PBS (pH = 7.3 at 25°C). The average increase in current for the rGO-nPt-nCe electrode was approximately 55% higher compared to a bare Pt/Ir electrode (n=3). The overpotential for the nanohybrid composite (+ 720 mV) was significantly lower than the bare electrode (+ 870 mV)

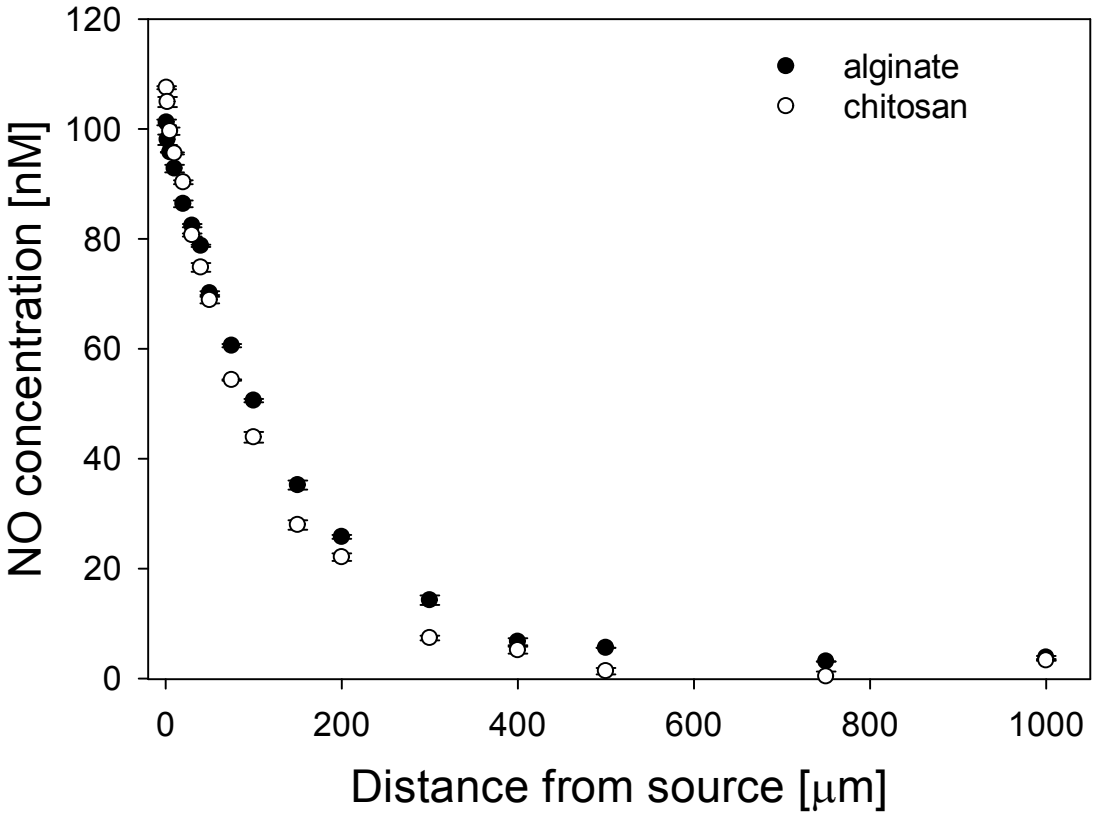

Figure S5. Concentration profiles recorded near source pipettes (200 μm tip diameter) constructed from the NO donor MAHMA NONOate and hydrogels. Effective diffusion coefficients were calculated from these profiles by minimizing the Chi^2 value between empirical data and the deterministic model shown in Equation 1. Concentration at the source pipette surface was within 2% of values obtained with a fiber optic UV spectrometer (337 nm)

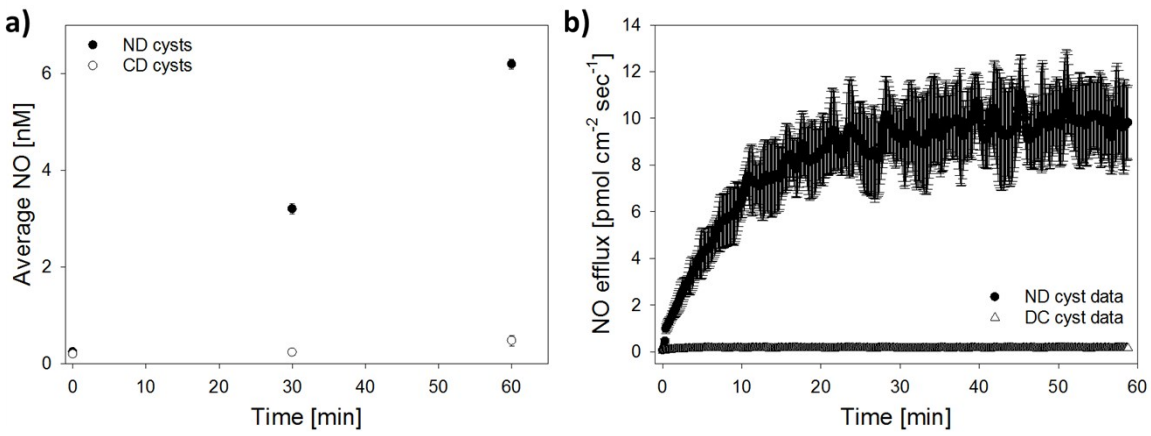

Figure S6. **a)** Average concentration at the surface *Artemia* cysts during exposure to 50mM exogenous hydrogen peroxide at time zero. **b)** NO efflux from ND and DC cysts after exposure to 50mM exogenous hydrogen peroxide at time zero.